Triggering of ground subsidence related fault motion in Mexico City by the M*w*8.2 Chiapas and the M*w*7.1 Puebla, September 2017 earthquakes.

D. Solano-Rojas[1], E. Havazli[1], E. Cabral-Cano[2], S. Wdowinski[3]

[1]*University of Miami, Rosenstiel School of Marine and Atmospheric Science.*
[2]*Instituto de Geofísica, Universidad Nacional Autónoma de México.*
[3]*Florida International University.*

geofisica UNAM

UNIVERSITY OF MIAMI ROSENSTIEL SCHOOL of MARINE & ATMOSPHERIC SCIENCE

FIU FLORIDA INTERNATIONAL UNIVERSITY

15 cities in central Mexico undergo rapid subsidence

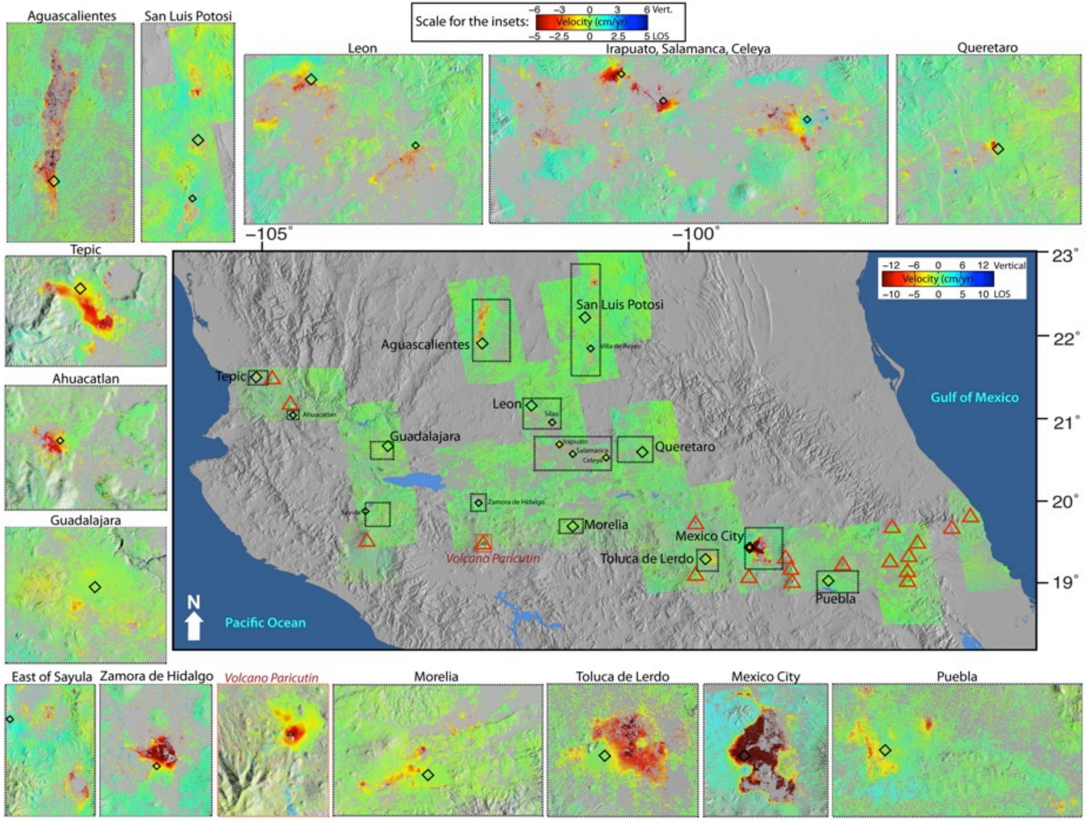

Chausssard et al., 2014

Angel de la Independencia, Mexico City.

Subsidence in Mexico City has been documented for over 100 yrs.

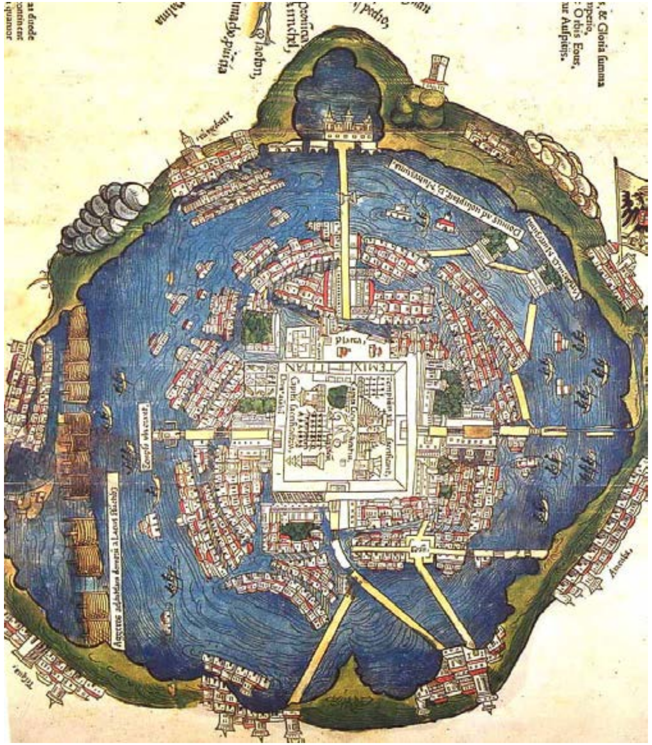

Mexico City (Tenochtitlan, the former Aztec capital) was built over the ancient Lake Texcoco beds (very high clay content).

Since its foundation in the 14th century Its relationship with this lacustrine system has been deeply intertwined and highly engineered.

This situation has presented severe challenges for all civil engineering and hydraulic projects.

Recurrent flooding in the XV century motivated the aztecs to build levees to prevent them.

Severe floodings in the XVI and XVII centuries were so devastating that a large part of its population died and even prompted the consideration of moving the capital elsewhere. It also initiated a 300 yr. long effort to artificially drain the basin.

The hydrological engineering to create a natural basin drainage started over 600 years ago and it is still an ongoing project

Nochistongo Canal

Artificially opened the basin and took over 100 yrs. to finish

Started operations	1788
Initial design	90 m^3/s
Current capacity	40 m^3/s

Grand Canal

Started operations	1910
Initial design	80 m^3/s
Current capacity	15 m^3/s

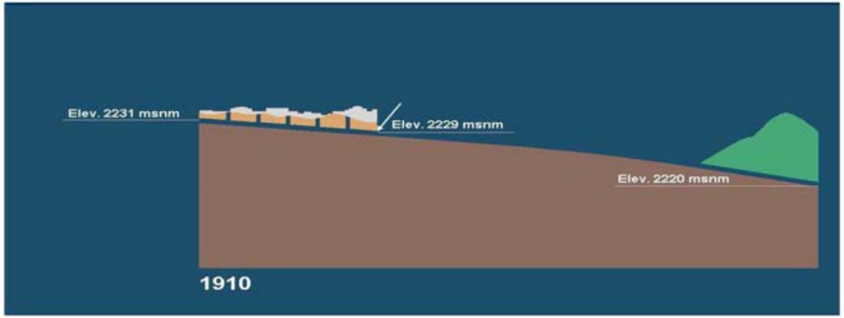

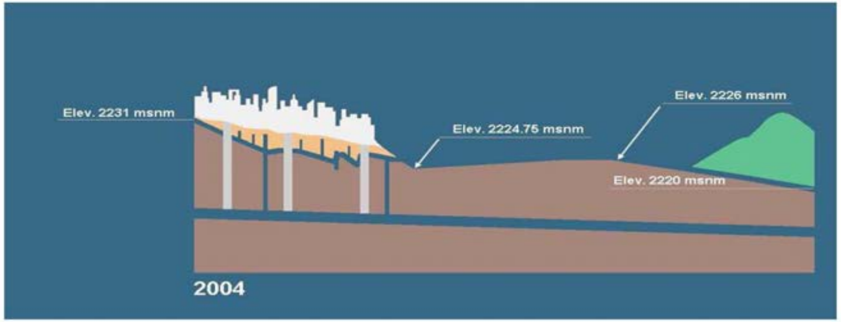


Inauguracion de los Vapores
entre
México y Chalco.
Banquete
en obsequio del
Sr. Presidente de la República
y sus Secretarios de Estado,
ofrecido por la Empresa.
MENU.
Mantequilla, Jamon, Salchichon, Aceitunas, Sardinas y Pepinos.
Caldo de pollo á la Sévigné.
Sopa de tortuga.
Pescado con salsa de ostiones.
Vol-au-vent de Lamprea.
Jamon americano con espinacas.
Filete de ternera á la Celini.
Pollo á la Tolosiana.
Costillas de cordero á la Primavera.
Pastel de liebre á la Jaletina.
Ponche de Kirsch.
Roastbeef á la inglesa.
Pavo asado.
Esparragos.
Chícharos á la Francesa.
Pasteles de frutas y á la Napolitana.
Crema al chocolate.
Jaletinas.
Pieza helada al Café.
Pastelitos.—Fruta.—Café y Thé.
Vinos.
Manzanilla. Jerez seco. Sauternes. Pommard. Volnay. Champagne Roederer. Cognac y Licores.
Chalco, Marzo 9 de 1890
Sr.

The environmental change has been so dramatic that our great grandfathers could still take a steam boat from the eastern section of the city to the city's downtown.

Something hard to believe nowadays...

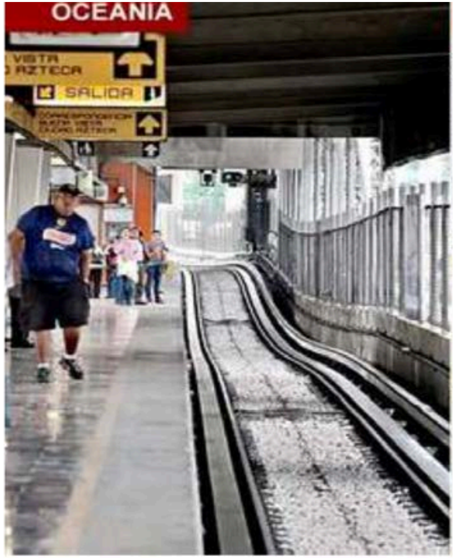

Subsidence effects include:

- Differential Subsidence
- Faulting
- Apparent emersion of structures

Photos: terra.com.mx

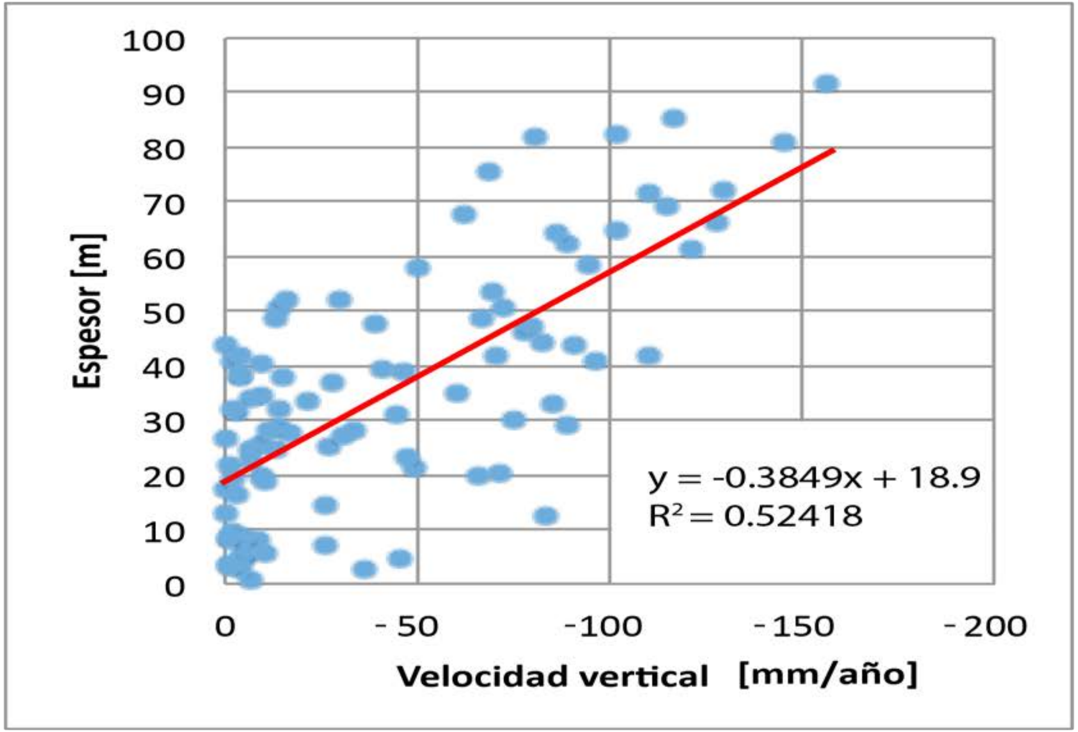

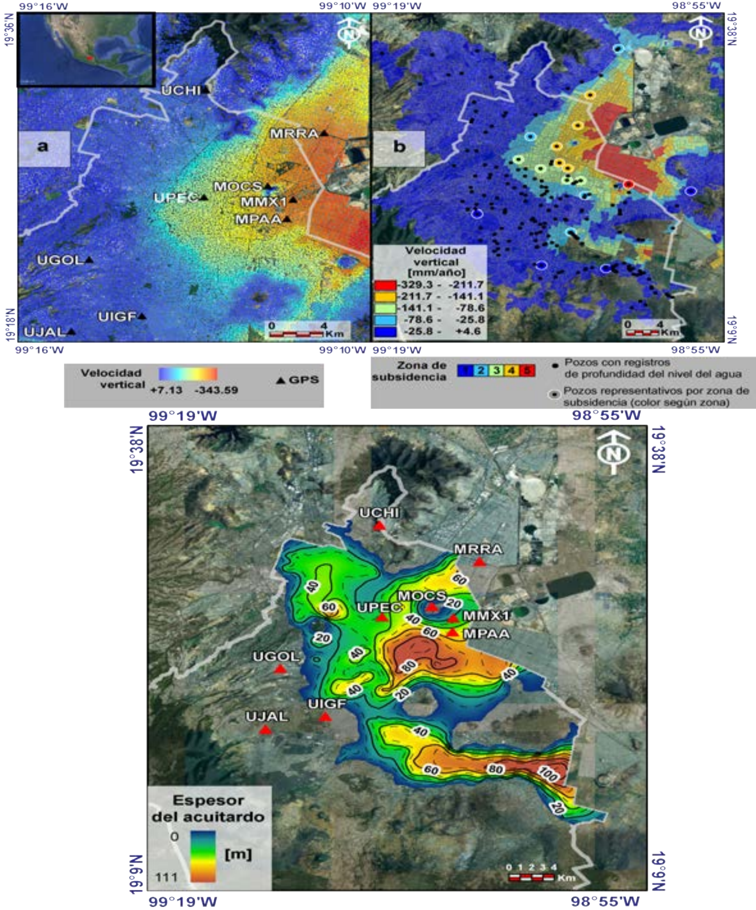

Solano-Rojas et. al. 2015.

In high subsiding areas, water well static level drawdown is well correlated to the aquifer thickness.

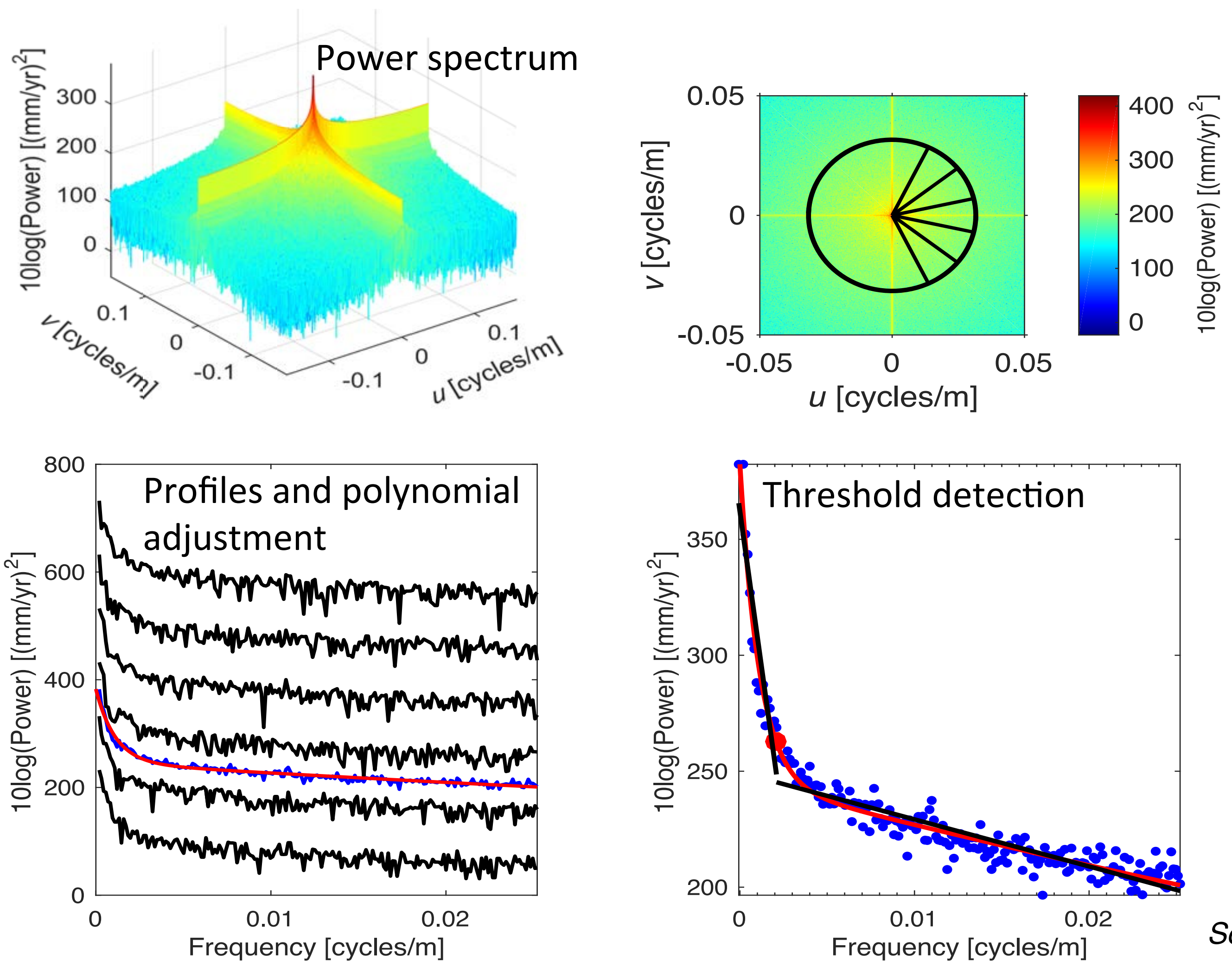

Analisis of spatial frequencies of the subsidence signal

Definition of wavelength thresholds that best describe the velocity subsidence.

Solano-Rojas, 2017, submitted.

This spatial frequency FFT filtering technique is capable of detecting new, subtle details that correspond to faults and anomalous structural behavour (aparent emersion).

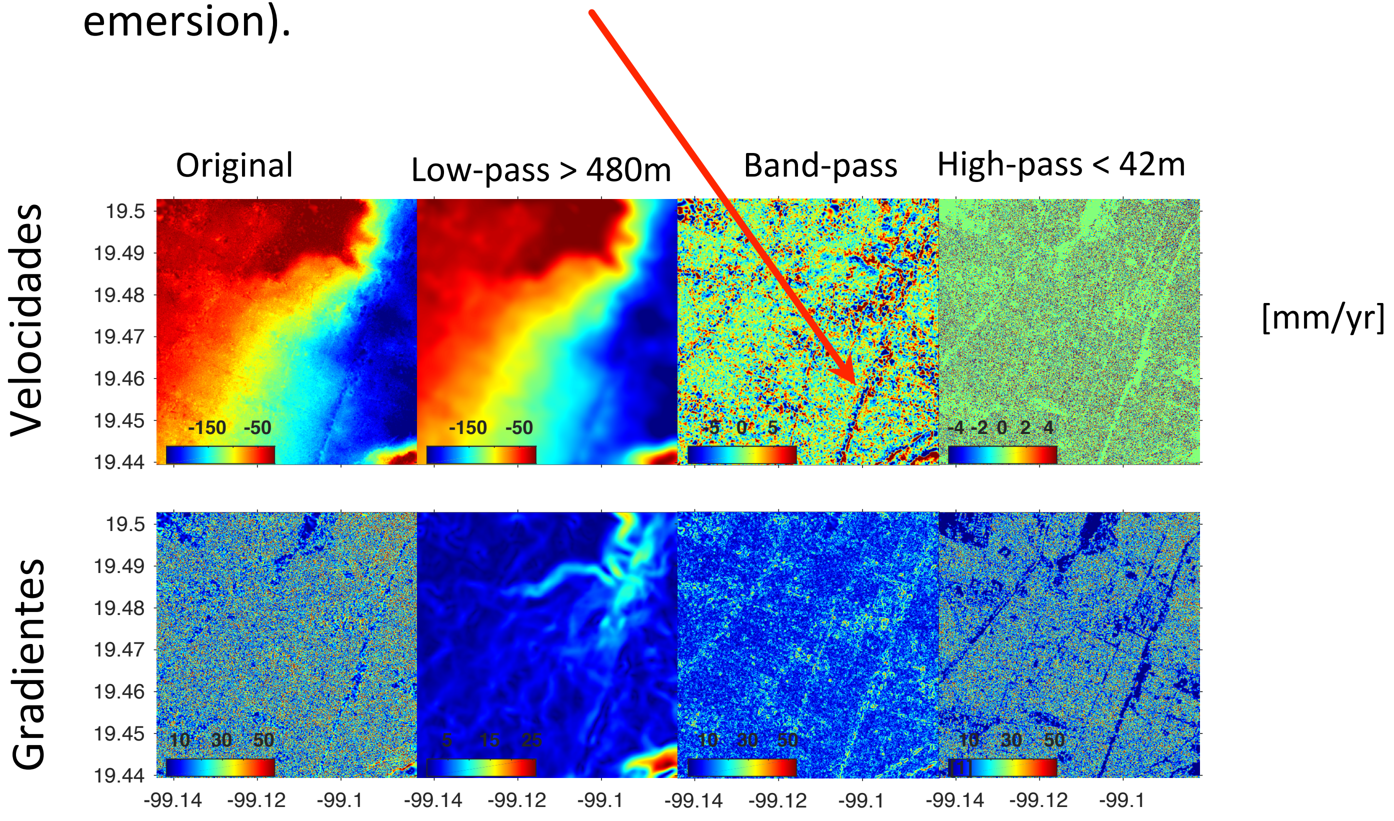

Solano-Rojas, 2017, submitted.

Detection of apparent emerion of large structures, such as large sewage works, overpasssses and Metro lines

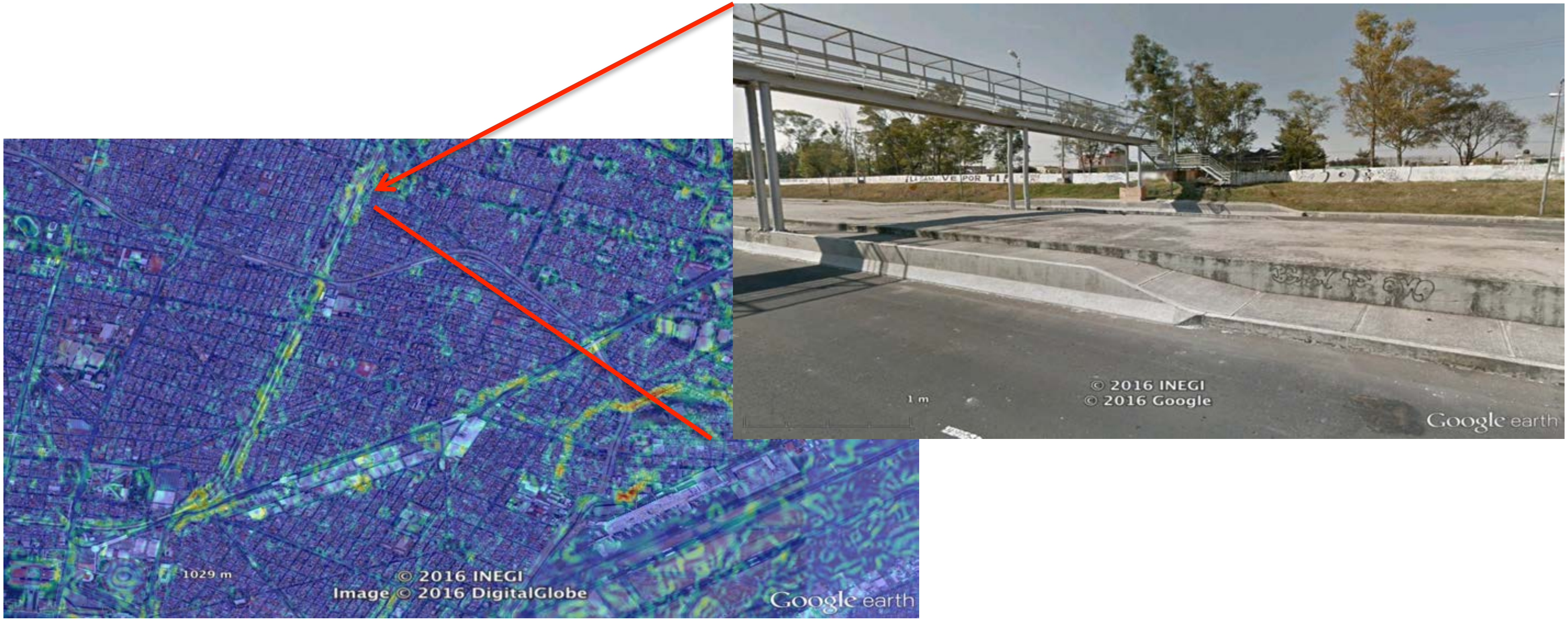

Solano-Rojas, 2017, submitted.

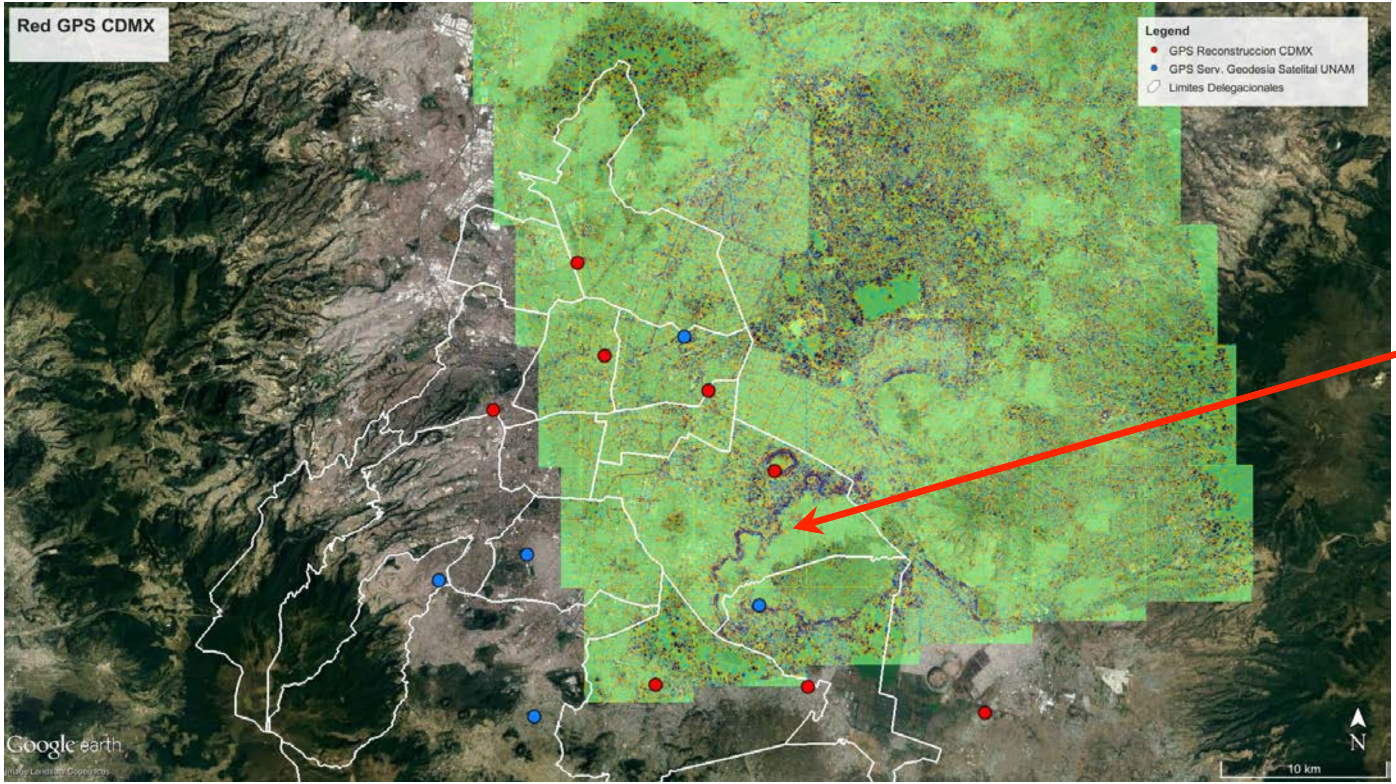

Detection of faults in the N, W and S slopes of Sierra Santa Catarina

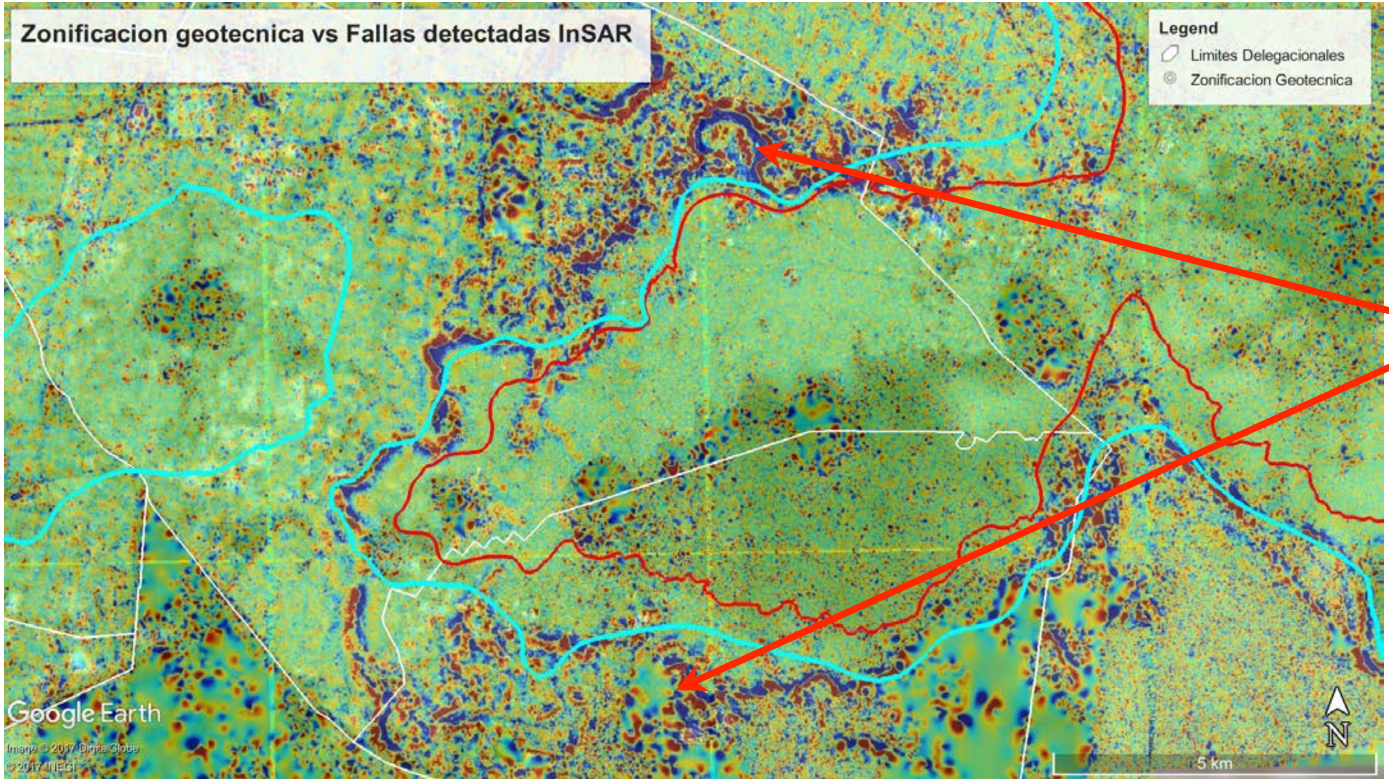

High fault density areas using this technique can be used to update and refine construction code and land use zoning.

Osmanoglu et al., 2011

Large structures undergo apparent emersion if its foundations are overcompensated.

They can be old colonial-era structures that have been reinforced with modern foundations such as the National Cathedral in Historic downtown, Mexico City

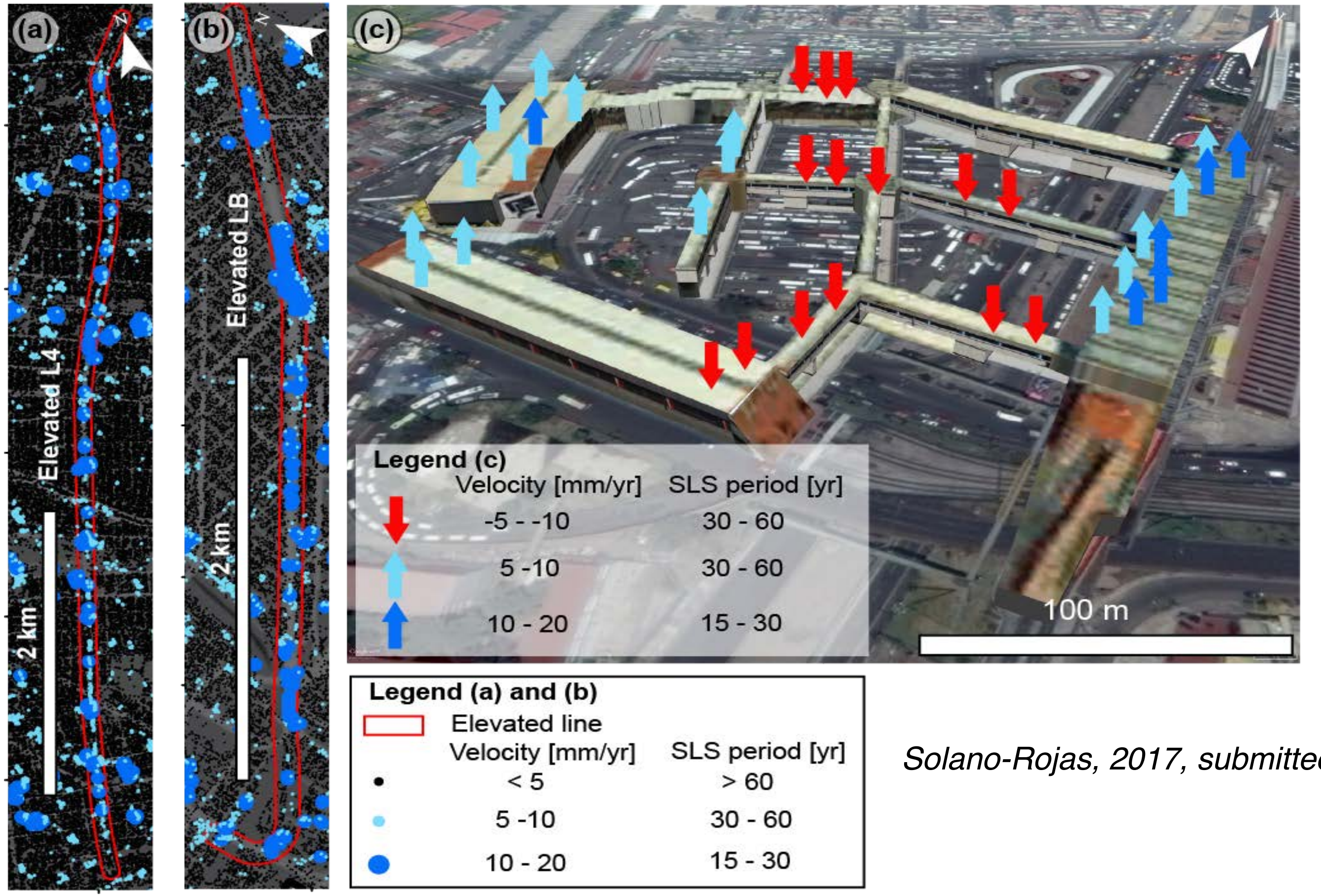

Solano-Rojas, 2017, submitted.

Modern structures such as Metro Lines 4, B and the Pantitlán station show apparent emersion

A Limit State estimation of the structure incicates reduction to ½ or ¼ of its serviceability life span.

This same method has proven very effective to detect subsidence−related faults

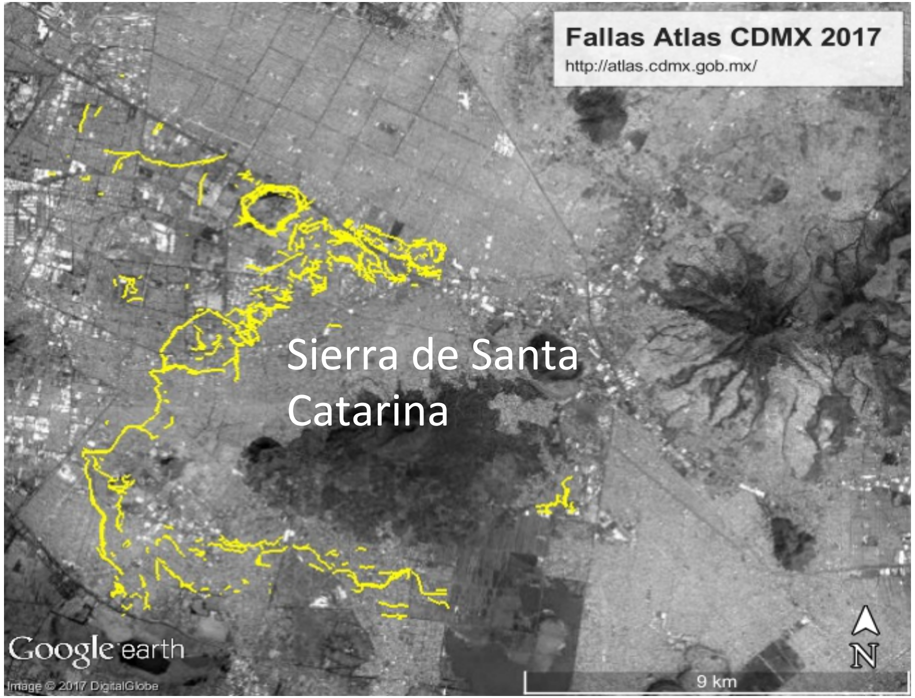

Field mapped faults (Atlas CDMX, 2017)

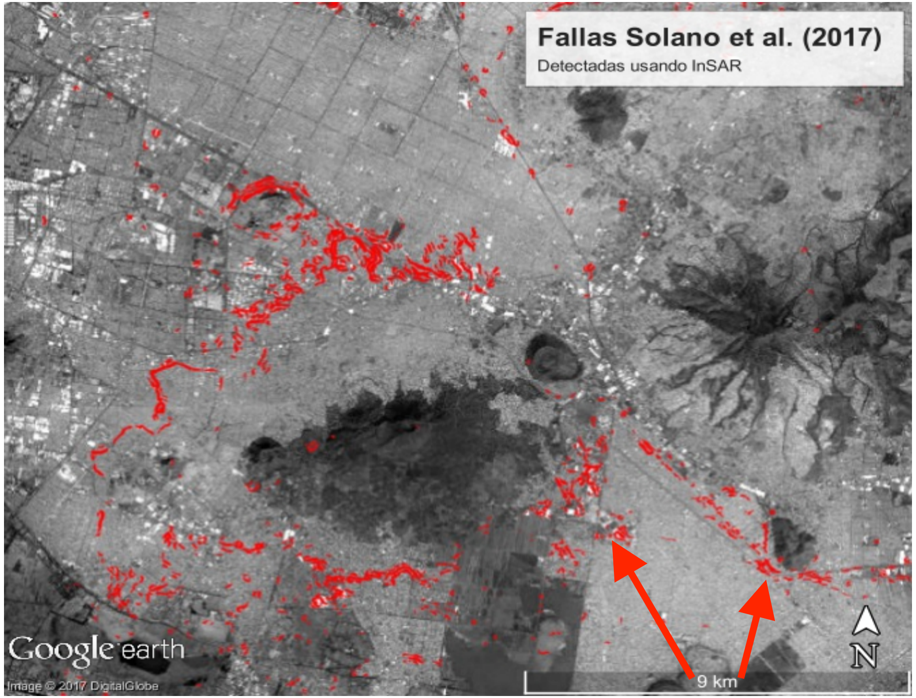

Fault detection using a spatial frequency filtering FFT technique

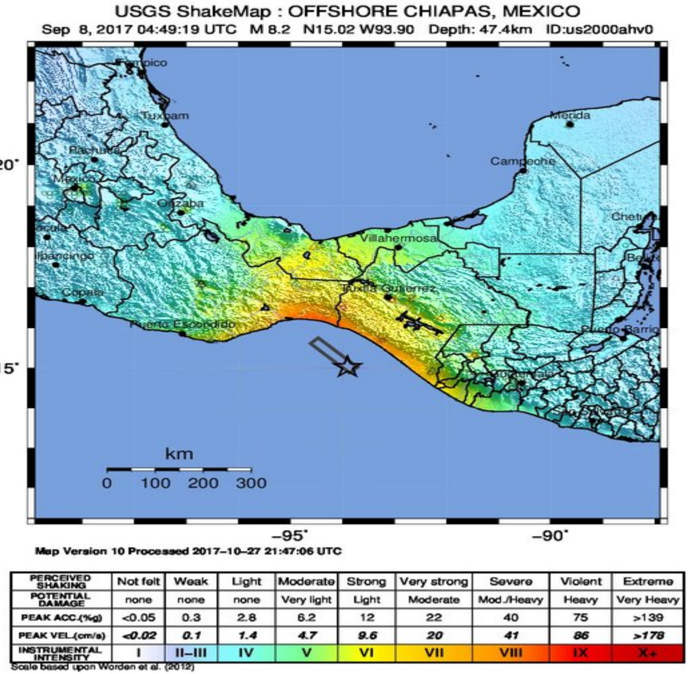

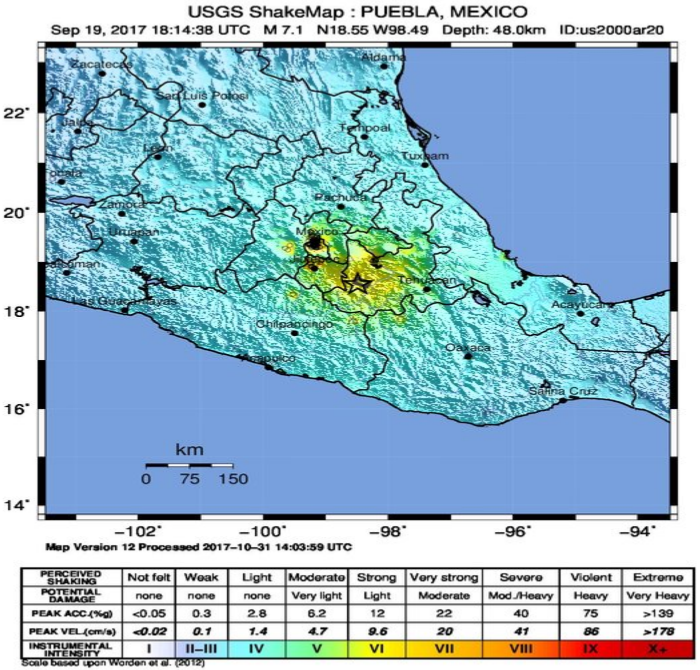

Shake Maps from September 7 and 19, 2017 earthquakes in Mexico. USGS

Mexico City recently experienced two large earthquakes only 11 days apart: the M*w*8.2 September 8th, 2017 with its epicenter offshore Chiapas, and the M*w*7.1 September 19th, 2017 with its epicenter in Puebla.

The M*w*8.2 earthquake was located over 700 km away from Mexico City and its effects in the city were not significant. However, the M*w*7.1 earthquake occurred only ~100 km away and produced severe damages.

T2 terminal, Mexico City International Airport

Photos of coseismic faulting taken after the Sept 19, 2017 central Mexico earthquake.

Earthquake damage locations

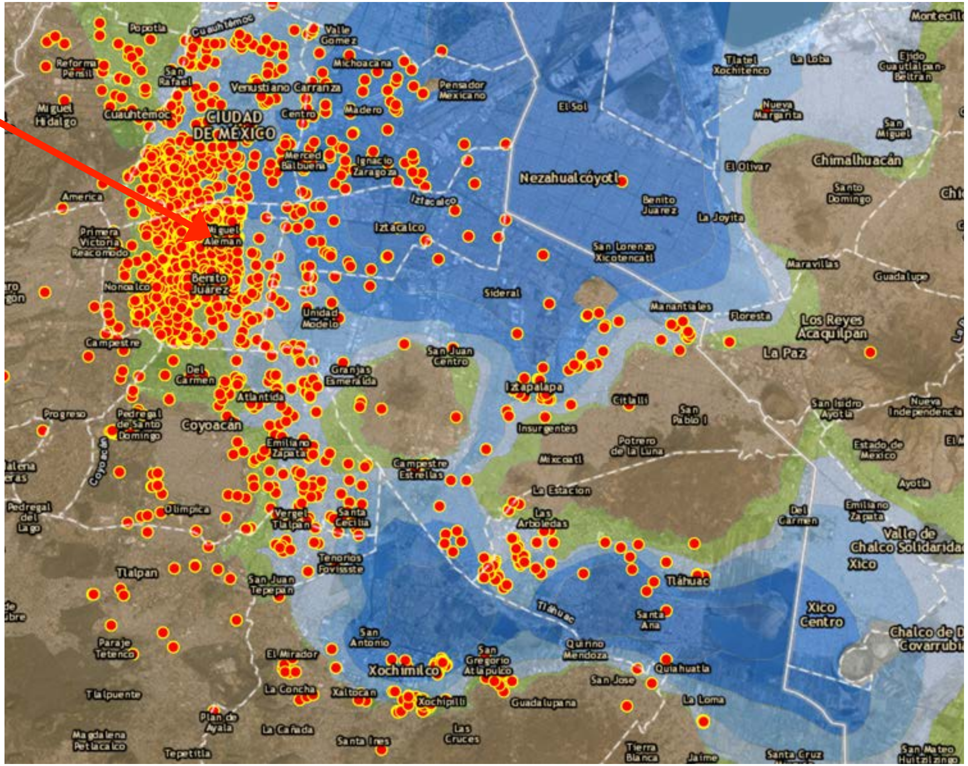

Grater seismic acceleration (site effect) affects buildings 6-10 floors high.

This explains damage in the western sector of the city.

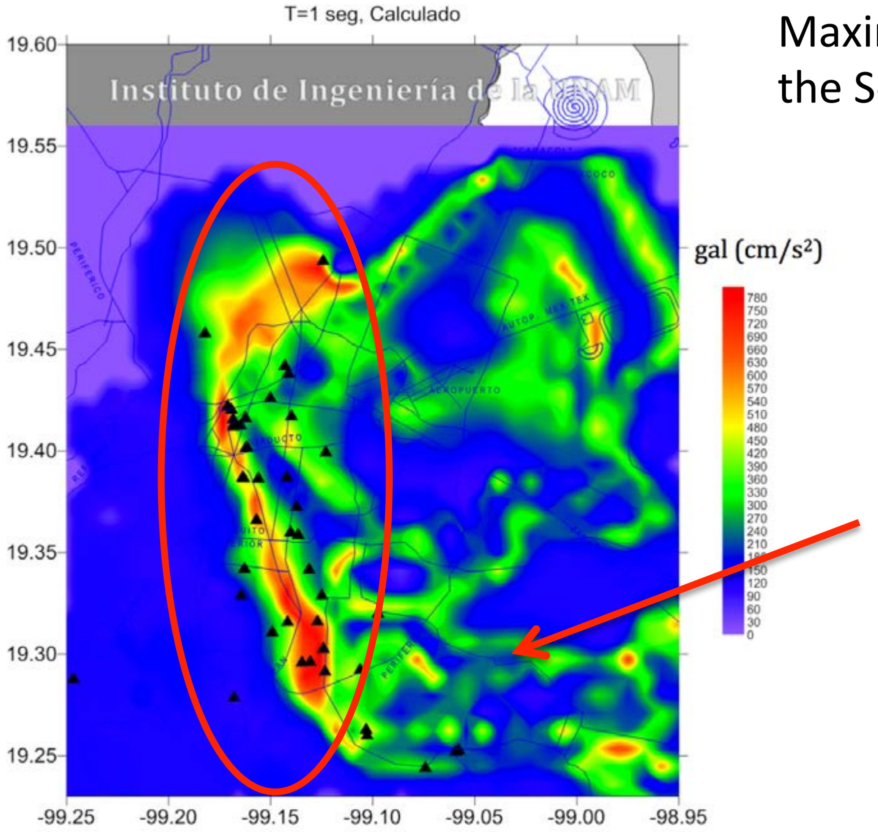

Maximum ground Acceleration during the Sept 19, 2017 earthquake.

But it doesn't explains much of the damage in the SE sector

Sentinel-1 InSAR analisis of subsidence acceleration for the Sept 7 and 19 earthquakes

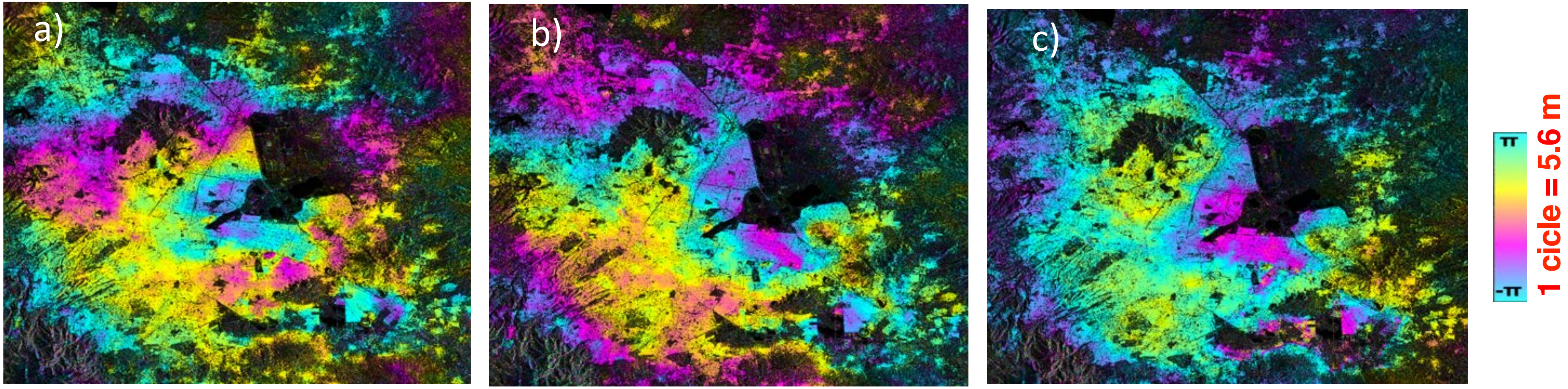

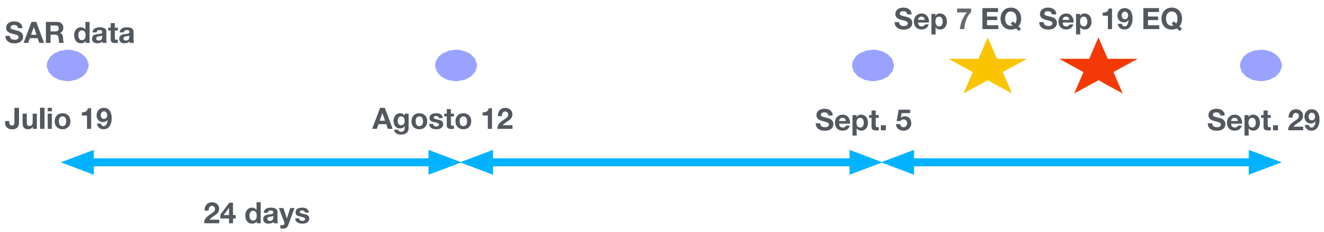

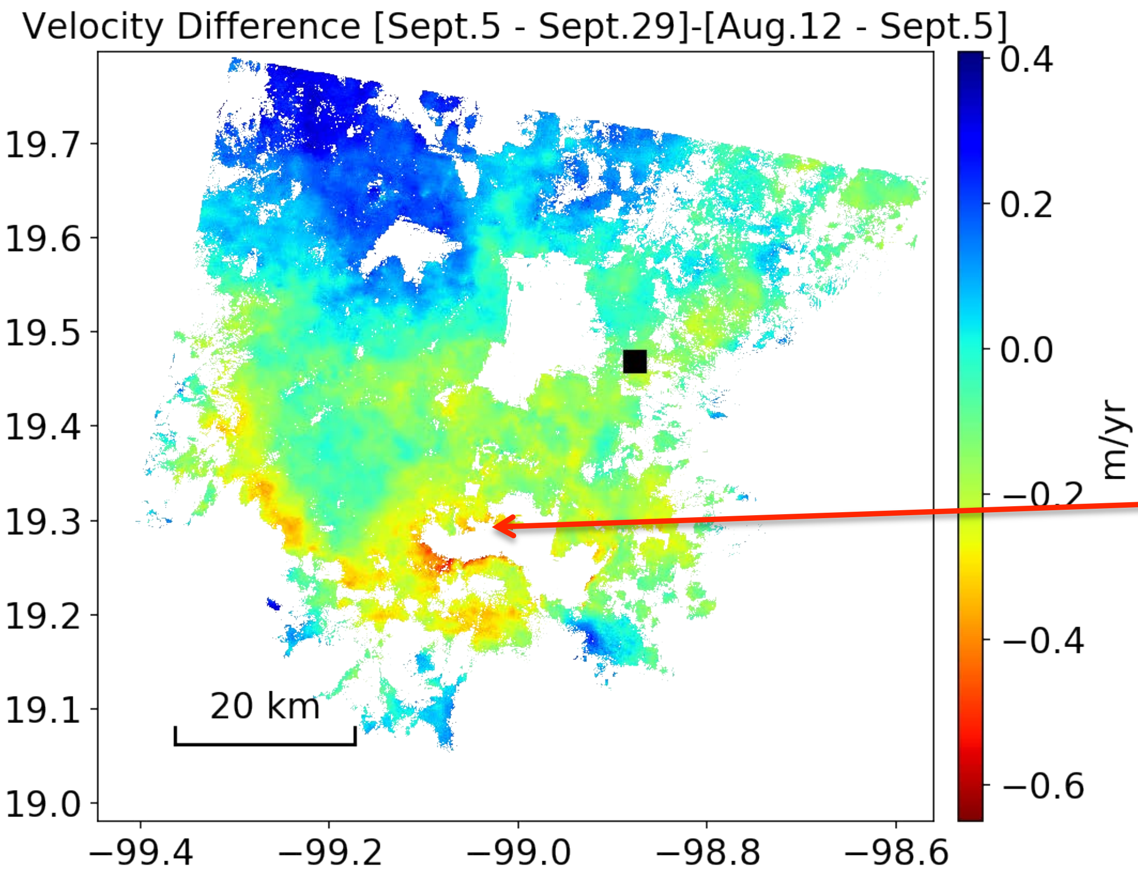

Unwrapping interferograms and subtracting the 24 day velocity field prior to the 2 earthquakes interferogram defines areas of subsidence acceleration due to the earthquakes

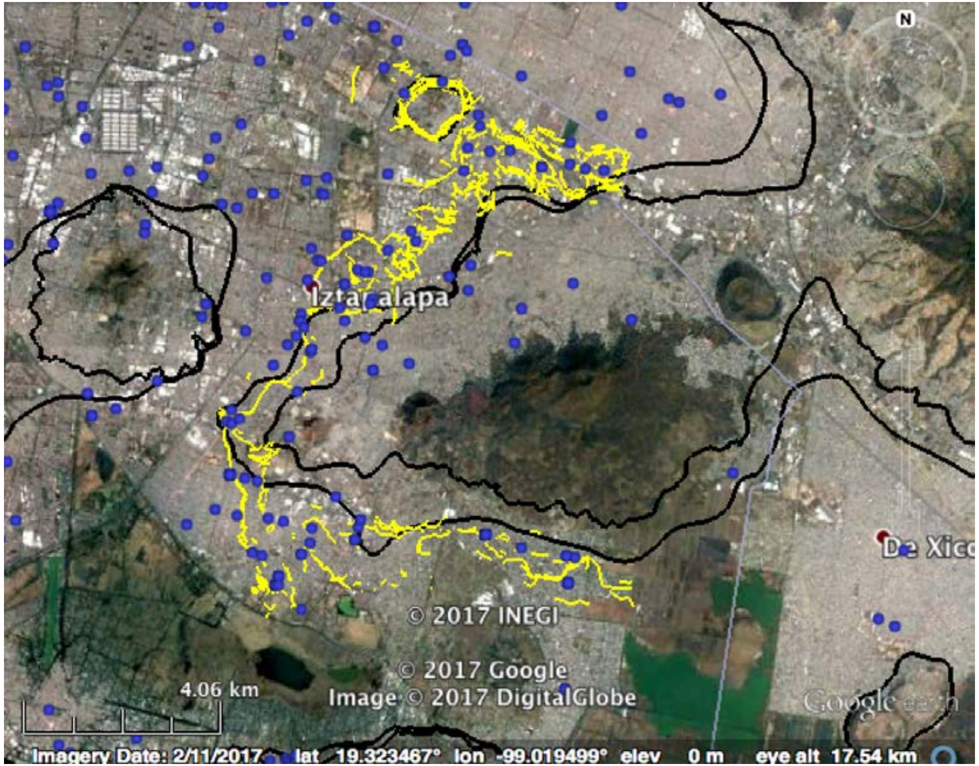

Reported structural damage (blue dots), and subsidence related faulting (yellow lines) coincide with these regions

Conclusions

A large portion of the reported damage in the southern sector of the city clearly correlates with the presence of pre-existent, subsidence-related faults that have been identified using spatial frequency FFT filtering (Solano-Rojas et. al, 2017).

A Sentinel-1 interferogram analysis, encompassing the integrated deformation for both the M*w*8.2 and M*w*7.1 earthquakes. shows that some subsiding areas underwent a rapid deformation in comparison to the previous interferograms, such as those from 24 and 48 days before.

The change in velocities and areal extent integrated during the seismic events, indicates that most of the seismically triggered deformation centred on high subsidence gradient areas in Mexico City.

We interpret that the energy released during these earthquakes is responsible for a distinctive deformation that is not shared by other sectors of the city where the underlying lacustrine sediment package is either thinner or absent.